

GEMINI Implementation Details

Matthew D. Zettergren, PhD
`matthew.zettergren@icloud.com`

April 8, 2023

Contents

1 GEMINI Model: Executive Summary	3
2 GEMINI Model Heritage	4
3 Internal Organization of GEMINI	6
4 GEMINI Source Code Repositories	6
5 Cmake Build System for GEMINI	7
6 Continuous Integration (CI)	7
6.1 Automatic CI	7
6.2 Comprehensive Continuous Integration (long CI)	7
7 GEMINI Data Structures	8
7.1 Mesh Objects	8
7.2 Inputdata Objects	8
7.3 Output Data Formats and Files	8
8 GEMINI Umbrella Library: libgemini	8

9	The trees-GEMINI Application	8
----------	-------------------------------------	----------

10	Validation with GNSS Data	9
-----------	----------------------------------	----------

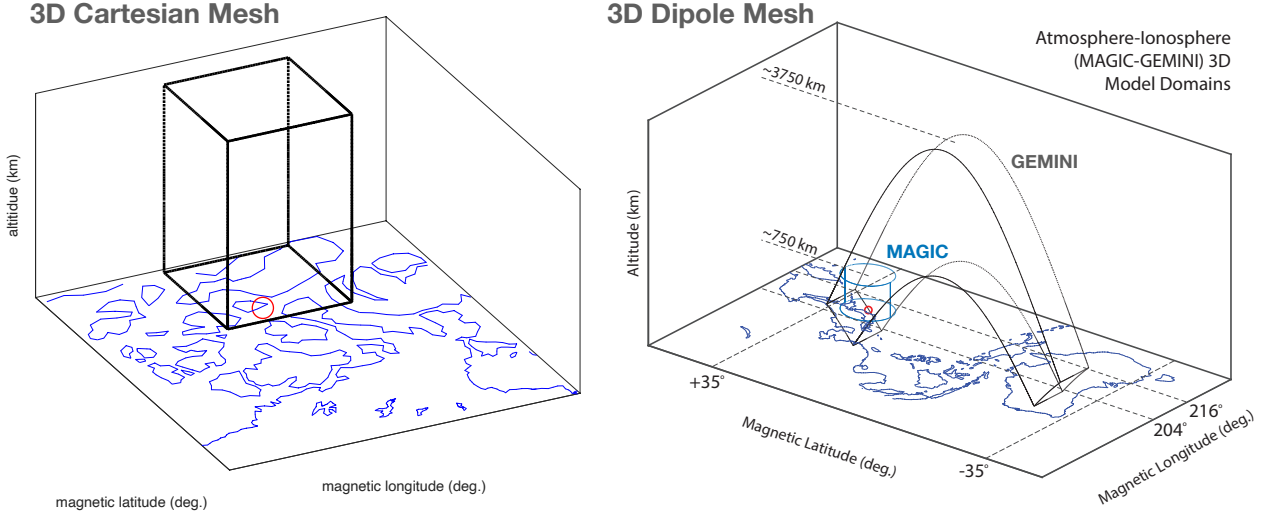


Figure 1: Examples of commonly used GEMINI mesh configurations: (left) a Cartesian mesh centered near the geomagnetic pole near Resolute Bay Canada, (right) an interhemispheric dipole mesh used with studies of infrasound and gravity wave impacts on the ionosphere.

1 GEMINI Model: Executive Summary

GEMINI: The “Geospace Environment Model for Ion-Neutral Interactions” is a 3D ionospheric model based on Zettergren and Semeter (2012), that has been applied in wide variety of ionospheric studies (Zettergren, op. cit.). The model uses a tilted dipole (Huba et al., 2000) or Cartesian mesh, and comprises a fluid system of equations (Schunk, 1977; Blelly and Schunk, 1993) describing dynamics of the ionospheric plasma, self-consistently coupled to a quasi-static (defined below) treatment of electrical currents. The fluid system is a set of three conservation equations (mass, parallel momentum, and energy) for each ionospheric species (Zettergren and Snively, 2015, Appendix A). Source terms in the continuity equations include photoionization Solomon and Qian (2005); Richards et al. (1994) and impact ionization via integration of the physics-based energetic electron transport model, GLOW (Solomon, 2001). Efficient semi-empirical methods for energy deposition calculations (Fang et al., 2008) can also be used. A full set of chemical reactions needed for the E- and F-regions is taken from Diloy et al. (1996); St-Maurice and Laneville (1998).

Perpendicular components of the plasma momentum equations in GEMINI are resolved via a quasi-static force balance approximation (Zettergren et al., 2015), viz. a static solution is applied but the parameters of the system (importantly conductivity) are allowed to change in time. Electric fields are found by enforcing a divergence-free current density, where the current consists of conduction, polarization, and pressure contributions (e.g. as in ?). This approach assumes a leading order electrostatic description supplemented by terms correcting for polarization currents from varying field structures (Mitchell et al., 1985) (i.e. ion inertial effects). Because the GEMINI solver is inherently (quasi-)static in nature it can be driven from either field-aligned current (FAC) or electric field conditions boundary conditions. Specifically, the ionospheric electric field is approximated by $\mathbf{E} = -\nabla\Phi$ but current closure solutions include ion inertial effects.

The use of a quasi-static solution notably omits Alfvén waves; however, many mesoscale structures are well-described as static (e.g. Lynch et al., 2015). Recent reviews suggest that alternating current (AC) Poynting flux is typically reported at lower levels than direct current (DC) Poynting flux, but can be highly variable; the relative importance of these two sources (DC vs. AC) is unknown (?). Our modeling focuses on the DC input effects (and particle inputs) as we argue this is the only part of the Poynting flux that can feasibly be captured by non-idealized models – resolving propagation of Alfvén waves in a cross-scale (meso-to-large), 3D ionosphere-thermosphere (plasma-neutral coupling) model is computationally infeasible for resolutions and grid extents that we target. At the very minimum, research suggests that the DC part of the incoming energy and momentum (stress) is a major (perhaps even the largest) contributor and our data-driven methodology permits us to evaluate the extent to which the observations are DC. As better computational resources and algorithms become available in the future it should be possible to begin to address AC portions of the spectrum, but that is not within the project scope.

GEMINI presently assumes that the geomagnetic field lines are equipotentials (a particularly good assumption for highly conducting situations likely to accompany precipitation) and employs a field line integration in the equation solved to describe conservation of charge (cf. Zettergren and Snively, 2015, Equation 1). Newer versions of GEMINI also include additional current terms needed for high-resolution modeling, like diamagnetic currents and diffusive transport perpendicular to \mathbf{B} .

2 GEMINI Model Heritage

The use of GEMINI for scientific applications is documented in a number of studies and associated refereed journal articles:

- Zettergren, M. and Semeter, J. (2012). Ionospheric plasma transport and loss in auroral downward current regions. *Journal of Geophysical Research: Space Physics*, 117(A6)
- Zettergren, M. and Snively, J. (2013). Ionospheric signatures of acoustic waves generated by transient tropospheric forcing. *Geophysical Research Letters*, 40(20):5345–5349
- Zettergren, M., Lynch, K., Hampton, D., Nicolls, M., Wright, B., Conde, M., Moen, J., Lessard, M., Miceli, R., and Powell, S. (2014). Auroral ionospheric f region density cavity formation and evolution: Mica campaign results. *Journal of Geophysical Research: Space Physics*, 119(4):3162–3178
- Zettergren, M. and Snively, J. (2015). Ionospheric response to infrasonic-acoustic waves generated by natural hazard events. *Journal of Geophysical Research: Space Physics*, 120(9):8002–8024
- Zettergren, M., Semeter, J., and Dahlgren, H. (2015). Dynamics of density cavities generated by frictional heating: Formation, distortion, and instability. *Geophysical Research Letters*, 42(23)
- Lynch, K., Hampton, D., Zettergren, M., Bekkeng, T., Conde, M., Fernandes, P., Horak, P., Lessard, M., Miceli, R., Michell, R., et al. (2015). Mica sounding rocket observations

of conductivity-gradient-generated auroral ionospheric responses: Small-scale structure with large-scale drivers. *Journal of Geophysical Research: Space Physics*, 120(11):9661–9682

- Perry, G., Dahlgren, H., Nicolls, M., Zettergren, M., St.-Maurice, J.-P., Semeter, J., Sundberg, T., Hosokawa, K., Shiokawa, K., and Chen, S. (2015). Spatiotemporally resolved electrodynamic properties of a sun-aligned arc over resolute bay. *Journal of Geophysical Research: Space Physics*, 120(11):9977–9987
- Burleigh, M. and Zettergren, M. (2017). Anisotropic fluid modeling of ionospheric upflow: Effects of low-altitude anisotropy and thermospheric winds. *Journal of Geophysical Research: Space Physics*, 122(1):808–827
- Swoboda, J., Semeter, J., Zettergren, M., and Erickson, P. J. (2017). Observability of ionospheric space-time structure with isr: A simulation study. *Radio Science*, 52(2):215–234
- Zettergren, M., Snively, J., Komjathy, A., and Verkhoglyadova, O. (2017). Nonlinear ionospheric responses to large-amplitude infrasonic-acoustic waves generated by undersea earthquakes. *Journal of Geophysical Research: Space Physics*, 122(2):2272–2291
- Burleigh, M., Heale, C., Zettergren, M., and Snively, J. (2018). Modulation of low-altitude ionospheric upflow by linear and nonlinear atmospheric gravity waves. *Journal of Geophysical Research: Space Physics*, 123(9):7650–7667
- Zettergren, M. and Snively, J. (2019). Latitude and longitude dependence of ionospheric tec and magnetic perturbations from infrasonic-acoustic waves generated by strong seismic events. *Geophysical Research Letters*, 46(3):1132–1140
- Burleigh, M., Zettergren, M., Lynch, K., Lessard, M., Moen, J., Clausen, L., Kenward, D., Hysell, D., and Liemohn, M. (2019). Transient ionospheric upflow driven by poleward moving auroral forms observed during the rocket experiment for neutral upwelling 2 (renu2) campaign. *Geophysical Research Letters*, 46(12):6297–6305
- Deshpande, K. B. and Zettergren, M. D. (2019). Satellite-beacon ionospheric-scintillation global model of the upper atmosphere (sigma) iii: Scintillation simulation using a physics-based plasma model. *Geophysical Research Letters*, 46(9):4564–4572
- Inchin, P., Snively, J., Zettergren, M., Komjathy, A., Verkhoglyadova, O., and Tulasi Ram, S. (2020). Modeling of ionospheric responses to atmospheric acoustic and gravity waves driven by the 2015 nepal 7.8 gorkha earthquake. *Journal of Geophysical Research: Space Physics*, 125(4):e2019JA027200
- Spicher, A., Deshpande, K., Jin, Y., Oksavik, K., Zettergren, M. D., Clausen, L. B., Moen, J. I., Hairston, M. R., and Baddeley, L. (2020). On the production of ionospheric irregularities via kelvin-helmholtz instability associated with cusp flow channels. *Journal of Geophysical Research: Space Physics*, 125(6):e2019JA027734
- Inchin, P., Snively, J., Kaneko, Y., Zettergren, M., and Komjathy, A. (2021). Inferring the evolution of a large earthquake from its acoustic impacts on the ionosphere. *AGU Advances*, 2(2):e2020AV000260

- Díaz Peña, J., Semeter, J., Nishimura, Y., Varney, R., Reimer, A., Hairston, M., Zettergren, M., Hirsch, M., Verkhoglyadova, O., Hosokawa, K., et al. (2021). Auroral heating of plasma patches due to high-latitude reconnection. *Journal of Geophysical Research: Space Physics*, 126(12):e2021JA029657
- Clayton, R., Burleigh, M., Lynch, K. A., Zettergren, M., Evans, T., Grubbs, G., Hampton, D. L., Hysell, D., Kaepller, S., Lessard, M., et al. (2021). Examining the auroral ionosphere in three dimensions using reconstructed 2d maps of auroral data to drive the 3d gemini model. *Journal of Geophysical Research: Space Physics*, 126(11):e2021JA029749
- Lamarche, L. J., Deshpande, K. B., and Zettergren, M. D. (2022). Observations and modeling of scintillation in the vicinity of a polar cap patch. *Journal of Space Weather and Space Climate*, 12:27
- Burleigh, M., Lynch, K., Zettergren, M., and Clayton, R. (2022). Spatiotemporal limitations of data-driven modeling: An isinglass case study. *Journal of Geophysical Research: Space Physics*, 127(9):e2021JA030242

These studies encapsulate a wide range of applications of the model from equatorial to low/mid-latitude and high-latitude and a number of studies where the model output has been critically compared against available data in validation exercises. Additional validation tests not yet published are included in later sections of this document. GEMINI's technology readiness level (TRL) is thus suggested as TRL6.

3 Internal Organization of GEMINI

MZ - top-level model connections

MZ - top level GEMINI module organization

MZ - example lower-level organization

MZ - example external libraries

4 GEMINI Source Code Repositories

Due to the large amount of source code, GEMINI is organized into about a dozen repositories ranging from core model numerical parts to scripts that allow one to build all external library dependencies.

5 Cmake Build System for GEMINI

MH - focus on current state and additions made during AIRWaveS

6 Continuous Integration (CI)

6.1 Automatic CI

The base `gemini3d` repository includes a set of integration and unit tests that can be run by a user upon compilation of model to test a number of model components as well as several integration tests that run simple model configurations and compare results against reference data archived in online repositories. These tests are also run via GitHub Actions anything a new update is pushed to the `gemini3d` repository. These test are designed to be able to run in a matter of minutes on a modest computer.

MH: cmake implementation details, locations of reference data, details of github actions and examples, descriptions of tests

example plots of output?

6.2 Comprehensive Continuous Integration (long CI)

Integration tests done by the automatic CI system are necessarily limited to those which can run quickly; yet there are a huge number of potential applications of the GEMINI model. A more comprehensive set of tests, in the `gemci` repository have been developed in order to check a number of other common use cases of the model against reference data. These include:

- Instability development utilizing periodic grids and quasi-dynamic solvers:
- Auroral electron precipitation and field-aligned currents:
- 2D and 3D cusp, open curvilinear grids with soft electron precipitation and field-aligned currents
- Closed, dipole grids with file input neutral perturbations:

A more complete description of each of these tests is given in the README file in the `gemci` repository under the `cfg` folder. The complete set of long CI tests is designed to be run in about 12 hours on a modest computer system.

MH: cmake implementation details, locations of ref. data

example plots of output?

7 GEMINI Data Structures

7.1 Mesh Objects

7.2 Inputdata Objects

7.3 Output Data Formats and Files

MH - h5fortran and output information

8 GEMINI Umbrella Library: libgemini

To allow maximum flexibility in how GEMINI functionality is used, we have developed a library containing core functionality that is accessible from applications written in fortran, C, and C++ languages.

MZ - Modularization of app-level implementation from numerical operations

MZ - Isolation of grid and solution data; toward allowing multiple patches on a single worker. There is a need in some applications for GEMINI to accommodate multiple independent sub-domains (with attendant grid and solution data) on a single mpi worker. This precludes use of any module-scope variables as these are limited to one per worker and required a full code refactor so that grid and solution data are always passed to numerical routines as procedure arguments (and not thru common blocks or module-scope variables).

MZ - C interoperability details

diagram illustrating parallelization using workers, patches, and AMR

9 The trees-GEMINI Application

A GEMINI application has been implemented under the forestclaw API in order to allow adaptive mesh refinement (AMR) using forestclaw’s three-dimensional, extruded mesh capabilities. EMINI applications using ForestClaw / p4est AMR, termed Trees-GEMINI, have recently been developed as part of Phase 1 of DARPA’s AtmoSense program. Our current setup uses GEMINI with an “extruded” mesh, whereby the AMR is done in two dimensions while the full extent of the third dimension is held on each computational “patch”. In Trees-GEMINI the extruded dimension is along geomagnetic field line which allows us to use existing implicit solvers for the numerically stiff electron thermal conduction process. Such solvers require all data along the parallel coordinate at once to function but are capable of dealing with the fast thermal conduction time scales (in

the electron population) while maintaining an otherwise reasonable time step for other explicit solutions for transport. Figure 2 shows a Trees-GEMINI simulation using multiply refined regions to model low-frequency acoustic wave propagation through the ionosphere using input from the MAGIC atmospheric dynamics model.

Trees-GEMINI currently contains most of the functionality of the core libGEMINI libraries including input data handling, dipole and Cartesian meshes, specifications of boundary conditions, fluid plasma solvers (chemistry, advection, diffusion), photoionization and impact ionization solvers, along with new output routines to optionally generate `vtk/vtu` files for efficient 3D visualization via the Paraview multi-platform open source application (Figure 2 shows an example). It currently does not have a AMR-capable (quasi-static) potential solution in the manner of the core GEMINI library as this functionality was not required by the projects that funded development of Trees-GEMINI. While the MAGIC data are historically input via files, a strategy for running the models side-by-side and exchanging data (one-way) thru memory is currently in development and testing as part of AtmoSense in a form that can, next, be reciprocated from GEMINI to MAGIC.

10 Validation with GNSS Data

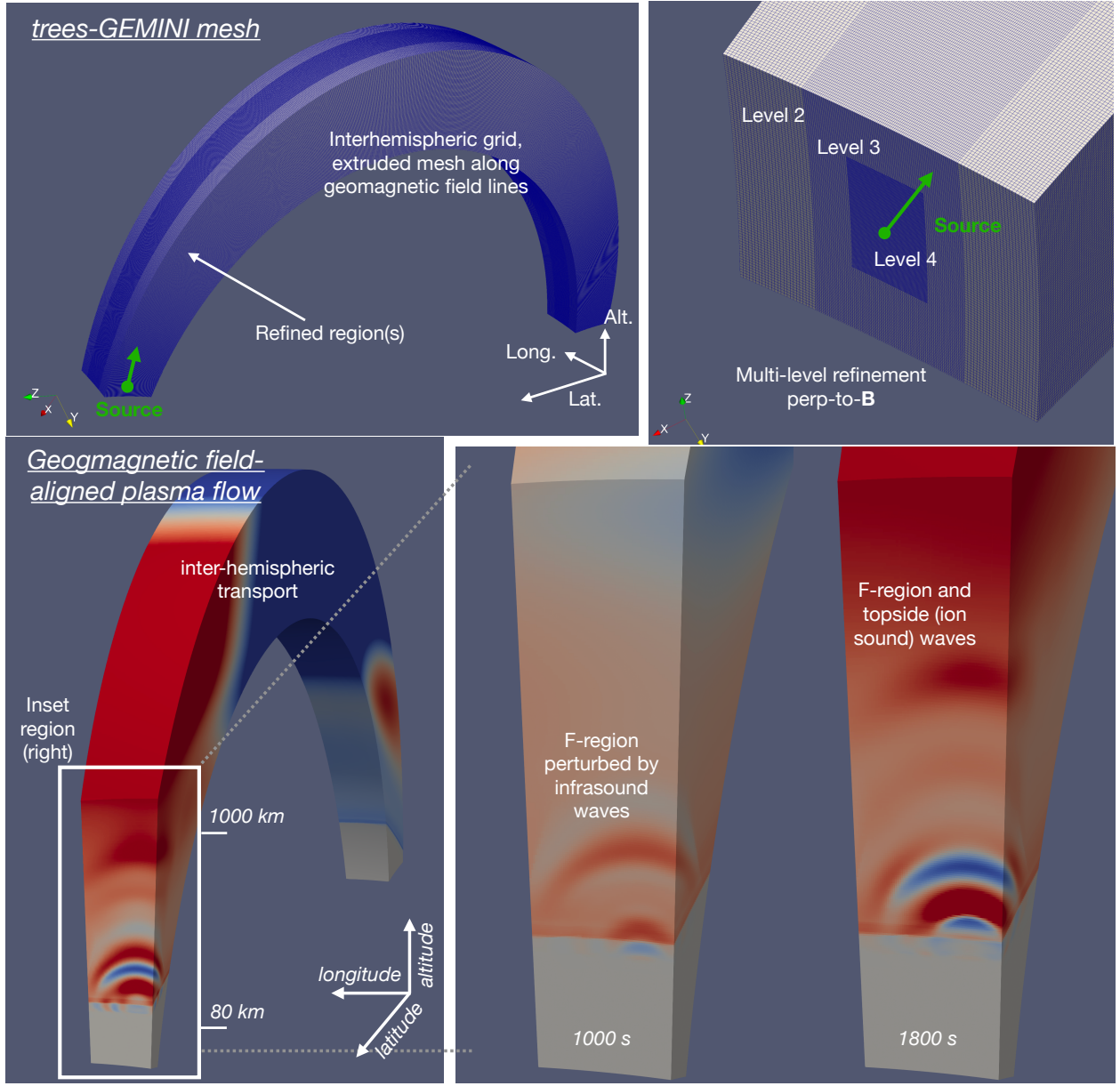


Figure 2: Trees-GEMINI simulation of mHz acoustic waves (AWs) propagating through the ionosphere using input data from MAGIC. (a,b) The overall grid and refinement structures used in the simulation, (c) the configuration of plasma flow, (d) individual output frame illustrating how AW forces ion flows in the F-region and topside.

References

- Blelly, P. and Schunk, R. (1993). A comparative study of the time-dependent standard 8-, 13-and 16-moment transport formulations of the polar wind. In *Annales geophysicae*, volume 11, pages 443–469. Copernicus.
- Burleigh, M., Heale, C., Zettergren, M., and Snively, J. (2018). Modulation of low-altitude ionospheric upflow by linear and nonlinear atmospheric gravity waves. *Journal of Geophysical Research: Space Physics*, 123(9):7650–7667.
- Burleigh, M., Lynch, K., Zettergren, M., and Clayton, R. (2022). Spatiotemporal limitations of data-driven modeling: An isinglass case study. *Journal of Geophysical Research: Space Physics*, 127(9):e2021JA030242.
- Burleigh, M. and Zettergren, M. (2017). Anisotropic fluid modeling of ionospheric upflow: Effects of low-altitude anisotropy and thermospheric winds. *Journal of Geophysical Research: Space Physics*, 122(1):808–827.
- Burleigh, M., Zettergren, M., Lynch, K., Lessard, M., Moen, J., Clausen, L., Kenward, D., Hysell, D., and Liemohn, M. (2019). Transient ionospheric upflow driven by poleward moving auroral forms observed during the rocket experiment for neutral upwelling 2 (renu2) campaign. *Geophysical Research Letters*, 46(12):6297–6305.
- Clayton, R., Burleigh, M., Lynch, K. A., Zettergren, M., Evans, T., Grubbs, G., Hampton, D. L., Hysell, D., Kaeppler, S., Lessard, M., et al. (2021). Examining the auroral ionosphere in three dimensions using reconstructed 2d maps of auroral data to drive the 3d gemini model. *Journal of Geophysical Research: Space Physics*, 126(11):e2021JA029749.
- Deshpande, K. B. and Zettergren, M. D. (2019). Satellite-beacon ionospheric-scintillation global model of the upper atmosphere (sigma) iii: Scintillation simulation using a physics-based plasma model. *Geophysical Research Letters*, 46(9):4564–4572.
- Díaz Peña, J., Semeter, J., Nishimura, Y., Varney, R., Reimer, A., Hairston, M., Zettergren, M., Hirsch, M., Verkhoglyadova, O., Hosokawa, K., et al. (2021). Auroral heating of plasma patches due to high-latitude reconnection. *Journal of Geophysical Research: Space Physics*, 126(12):e2021JA029657.
- Diloy, P.-Y., Robineau, A., Lilenstein, J., Blelly, P.-L., and Fontanari, J. (1996). A numerical model of the ionosphere, including the e-region above eiscat. In *Annales Geophysicae*, volume 14, pages 191–200. Springer.
- Fang, X., Randall, C. E., Lummerzheim, D., Solomon, S. C., Mills, M. J., Marsh, D. R., Jackman, C. H., Wang, W., and Lu, G. (2008). Electron impact ionization: A new parameterization for 100 ev to 1 mev electrons. *Journal of Geophysical Research: Space Physics*, 113(A9).
- Huba, J., Joyce, G., and Fedder, J. (2000). Sami2 is another model of the ionosphere (sami2): A new low-latitude ionosphere model. *Journal of Geophysical Research: Space Physics*, 105(A10):23035–23053.

- Inchin, P., Snively, J., Kaneko, Y., Zettergren, M., and Komjathy, A. (2021). Inferring the evolution of a large earthquake from its acoustic impacts on the ionosphere. *AGU Advances*, 2(2):e2020AV000260.
- Inchin, P., Snively, J., Zettergren, M., Komjathy, A., Verkhoglyadova, O., and Tulasi Ram, S. (2020). Modeling of ionospheric responses to atmospheric acoustic and gravity waves driven by the 2015 nepal 7.8 gorkha earthquake. *Journal of Geophysical Research: Space Physics*, 125(4):e2019JA027200.
- Lamarche, L. J., Deshpande, K. B., and Zettergren, M. D. (2022). Observations and modeling of scintillation in the vicinity of a polar cap patch. *Journal of Space Weather and Space Climate*, 12:27.
- Lynch, K., Hampton, D., Zettergren, M., Bekkeng, T., Conde, M., Fernandes, P., Horak, P., Lessard, M., Miceli, R., Michell, R., et al. (2015). Mica sounding rocket observations of conductivity-gradient-generated auroral ionospheric responses: Small-scale structure with large-scale drivers. *Journal of Geophysical Research: Space Physics*, 120(11):9661–9682.
- Mitchell, H., Fedder, J., Keskinen, M., and Zalesak, S. (1985). A simulation of high latitude f-layer instabilities in the presence of magnetosphere-ionosphere coupling. *Geophysical research letters*, 12(5):283–286.
- Perry, G., Dahlgren, H., Nicolls, M., Zettergren, M., St.-Maurice, J.-P., Semeter, J., Sundberg, T., Hosokawa, K., Shiokawa, K., and Chen, S. (2015). Spatiotemporally resolved electrodynamic properties of a sun-aligned arc over resolute bay. *Journal of Geophysical Research: Space Physics*, 120(11):9977–9987.
- Richards, P., Fennelly, J., and Torr, D. (1994). Euvac: A solar euv flux model for aeronomics calculations. *Journal of Geophysical Research: Space Physics*, 99(A5):8981–8992.
- Schunk, R. (1977). Mathematical structure of transport equations for multispecies flows. *Reviews of Geophysics*, 15(4):429–445.
- Solomon, S. C. (2001). Auroral particle transport using monte carlo and hybrid methods. *Journal of Geophysical Research: Space Physics*, 106(A1):107–116.
- Solomon, S. C. and Qian, L. (2005). Solar extreme-ultraviolet irradiance for general circulation models. *Journal of Geophysical Research: Space Physics*, 110(A10).
- Spicher, A., Deshpande, K., Jin, Y., Oksavik, K., Zettergren, M. D., Clausen, L. B., Moen, J. I., Hairston, M. R., and Baddeley, L. (2020). On the production of ionospheric irregularities via kelvin-helmholtz instability associated with cusp flow channels. *Journal of Geophysical Research: Space Physics*, 125(6):e2019JA027734.
- St-Maurice, J.-P. and Laneville, P. (1998). Reaction rate of o+ with o₂, n₂, and no under highly disturbed auroral conditions. *Journal of Geophysical Research: Space Physics*, 103(A8):17519–17521.
- Swoboda, J., Semeter, J., Zettergren, M., and Erickson, P. J. (2017). Observability of ionospheric space-time structure with isr: A simulation study. *Radio Science*, 52(2):215–234.

- Zettergren, M., Lynch, K., Hampton, D., Nicolls, M., Wright, B., Conde, M., Moen, J., Lessard, M., Miceli, R., and Powell, S. (2014). Auroral ionospheric f region density cavity formation and evolution: Mica campaign results. *Journal of Geophysical Research: Space Physics*, 119(4):3162–3178.
- Zettergren, M. and Semeter, J. (2012). Ionospheric plasma transport and loss in auroral downward current regions. *Journal of Geophysical Research: Space Physics*, 117(A6).
- Zettergren, M., Semeter, J., and Dahlgren, H. (2015). Dynamics of density cavities generated by frictional heating: Formation, distortion, and instability. *Geophysical Research Letters*, 42(23).
- Zettergren, M. and Snively, J. (2013). Ionospheric signatures of acoustic waves generated by transient tropospheric forcing. *Geophysical Research Letters*, 40(20):5345–5349.
- Zettergren, M. and Snively, J. (2015). Ionospheric response to infrasonic-acoustic waves generated by natural hazard events. *Journal of Geophysical Research: Space Physics*, 120(9):8002–8024.
- Zettergren, M. and Snively, J. (2019). Latitude and longitude dependence of ionospheric tec and magnetic perturbations from infrasonic-acoustic waves generated by strong seismic events. *Geophysical Research Letters*, 46(3):1132–1140.
- Zettergren, M., Snively, J., Komjathy, A., and Verkhoglyadova, O. (2017). Nonlinear ionospheric responses to large-amplitude infrasonic-acoustic waves generated by undersea earthquakes. *Journal of Geophysical Research: Space Physics*, 122(2):2272–2291.